

GROWTH AND STRUCTURE OF SnO/ZnO BIAxIAL NANOWIRES ON ZnO NANOWIRE BY VAPOR-LIQUID-SOLID MECHANISM

Tien Hung Pham¹, Quang Dat Tran¹, Xuan Thau Nguyen¹,
Vu Tung Nguyen¹, Tien Anh Nguyen¹, Van Thin Pham^{1,*}

¹Faculty of Physical and Chemical Engineering, Le Quy Don Technical University, Hanoi, Vietnam

Abstract

In this work, the biaxial SnO/ZnO nanowires in the average length of 5 μm , have been successfully synthesized on a ZnO-nanowire substrate using a chemical vapor deposition (CVD) system through a two-step process. First, ZnO nanowires were grown directly on the glass substrate with a gold catalyst. Then, these nanowires were used as templates for the growth of biaxial SnO/ZnO nanowires without any catalyst. The obtained products were characterized by X-ray diffraction (XRD), field-emission electron scanning microscopy (FE-SEM), and high-resolution transmission electron microscopy (HR-TEM). The Sn-Zn alloy formulated during the process was believed a catalyst for the growth of the biaxial SnO/ZnO nanowires. The biaxial structure was formed due to simultaneous growth of SnO and ZnO nanowire along the direction of SnO [110] and ZnO [002], respectively. A possible growth mechanism of the biaxial SnO/ZnO nanowire was discussed based on the vapor-liquid-solid (VLS) mechanism. The as-synthesized structure could be a good candidate for nano-sensors.

Keywords: SnO; ZnO; biaxial nanowires; CVD; VLS.

1. Introduction

In the past decades, metal oxide nanomaterials with special morphologies have attracted significant attention because their size and morphology have a strong influence on properties that are different from their bulk counterpart. Among these oxides, stannous oxide (SnO), an important p-type semiconductor with a direct optical band gap of 2.5-3.4 eV [1], has attracted considerable attention owing to its potential application in various fields, such as a catalyst [2], a coating substance [3], a thin film transistor (TFT) [4], an anode material for lithium-ion batteries [5, 6], a gas sensor [7, 8] and a precursor for the fabrication of SnO₂ [9]. Especially, SnO is unstable thermodynamically above 543 K, and the disproportionation and oxidation reactions of SnO are easily progressed under redox or inert atmosphere conditions [10]. Therefore, it was not easy to synthesize high purity SnO nanomaterials. Up to now, various morphologies of SnO have been synthesized such as diskettes [11], nanoplates [12], nanobranches [13], nanowhisker [14], nanosheets [15], nanoflowers [16], meshes [17], nanobelts and nanospheres [18] through a few synthetic routes such as sol-gel

* Email: thinpv@lqdtu.edu.vn

method [19], thermal decomposition [13], chemical vapor deposition (CVD) [20], hydrothermal method [12]. Among them, the ones based on thermal evaporation appear to be interesting due the simplicity of the method as well as its low cost and the good quality of the material obtained which usually grows following a vapor-solid (VS) or a vapor-liquid-solid (VLS) mechanism. Hybrid nanostructure from different nanomaterials are attracting increasing attention due to the possibility of tuning their chemical, electronic, and optical properties over a wide range. So far, research has focused on the one dimensional (1D) heterostructure with modulated compositions and interfaces have recently become of particular interest with respect to potential applications in nanoscale electronics and photonics [21]. Recently, 1-D p-type metals oxide semiconductor functionalized ZnO nanowires have gained great attentions since band alignment of these structures separate the charge carriers, electrons and holes, into different regions and thus may enhance the carrier lifetime. They have been intensively studied due to their wide applicability. For example, core-shell structure p-CuO/n-ZnO core-shell nanowires [22], p-SnO/n-ZnO string-like [23], p-Cr₂O₃/n-ZnO nanorods [24]; and p-NiO/n-ZnO [25] have used to improve sensing and application of photoluminescence. To the best of our knowledge, up to this moment, there are still rare reports in the literature on the synthesis of biaxial nanowires on the metal oxide nanowire. In a previous our study, the biaxial p-SnO/n-ZnO heterostructured nanowires were grown directly on the glass substrate using CVD system through one step process [26]. In this study, we introduce a process to synthesize biaxial SnO/ZnO nanowires on the ZnO nanowire using CVD system through two-step process. The microstructure and morphological properties based on biaxial nanowire structure were analyzed by XRD, FE-SEM and HR-TEM, respectively. Furthermore, details of the growth mechanism and formation of the biaxial nanowires are discussed.

2. Experiment

2.1. Synthesis of ZnO nanowires

A typical process for synthesizing the ZnO nanowires is mentioned as follows: First, glass substrates (with size of 1×2 cm²) were ultrasonically cleaned in acetone, ethanol and distilled water bath for 10 min, sequentially. Then, the sampling was directly sputter-coated with 5-nm-thick Au layer and was inserted on the quartz plate which were placed downstream. The glass substrate is 20 cm away from the source which was mixed from active carbon and ZnO powder (both purities are 99.99%) in a 1:1 weight ratio. The source put in an alumina boat and was loaded at the center of a quartz tube. After the quartz tube was evacuated to ~ 5×10⁻³ Torr, the furnace temperature was increased from room temperature to 950°C. When the temperature

increased up to growth temperature (950°C), a mixed gas of N₂-O₂ (N₂: 4 sccm, O₂: 1 sccm) was provided as the reaction gas. While introducing the reaction gas, the pressure of the system was maintained at 2×10^{-2} Torr and the temperature was kept at 950°C for 1 h. After the reaction, the furnace was naturally cool down to room temperature and the ZnO nanowires were collected on the glass substrate. These samples were used as the substrate for the second step.

2.2. Synthesis of branches ZnO/SnO biaxial nanowire

The biaxial SnO/ZnO nanowire heterostructures were synthesized in a closed tube furnace illustrated as Fig. 1. The ZnO nanowires substrate was placed on the quartz plate (20×3 cm²) which were placed downstream at the sampling points at a temperature of 360°C as shown in the Fig. 1. The SnO powder source (purity is 99.99%) were loaded at the center of a quartz tube in an alumina boat. Subsequently, the quartz tube was evacuated to 5×10^{-3} Torr and purged several times with high purity N₂ gas. After that the furnace temperature was increased from room temperature to 800°C and maintained at decomposition temperature for 1 h. During the reaction, no gas was introduced into tube and the pressure inside the quartz tube was kept at 5×10^{-3} Torr. After the deposition, the furnace could naturally cool down to room temperature and substrate with a gray film were then obtained.

2.3. Characterization

The morphologies of as-synthesized samples were analyzed by the field emission scanning electron microscopy (FE-SEM – JSM-6701F) operating at the accelerating of 10 kV. The phase, crystallinities, and chemical compositions of the samples were examined by means of X-ray diffraction (XRD) utilizing a CuK α radiation at $\lambda = 1.54178 \text{ \AA}$, potential of 40 kV and current of 30 mA and a high-resolution transmission electron microscopy (HR-TEM; Telnai G2F20S-BIAXIAL; Philips) attached with an energy dispersive (EDX) spectrometer. The elemental maps and line-scan profiles were measured in the scanning transmission electron microscopy mode (STEM) under an accelerated voltage of 200 kV.

3. Results and discussion

3.1. Characterization of the chemical vapor transport (CVT) products

Figure 2a shows a low-magnification FE-SEM image of ZnO nanowire networks are uniform. The higher magnification FE-SEM image in Fig. 2b show that ZnO nanowires with smooth surface and uniform diameters of ~80 nm. In addition, the catalyst

droplets were found at the tips of the nanowire, implying that the growth of the ZnO nanowires may follow the VLS mechanism with Au catalyst [27].

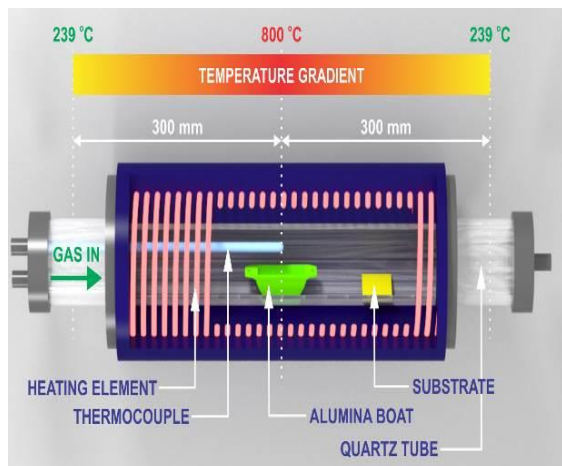


Fig. 1. Schematic diagram of the system employed for the synthesis of SnO/ZnO biaxial nanowires on the ZnO NW substrate.

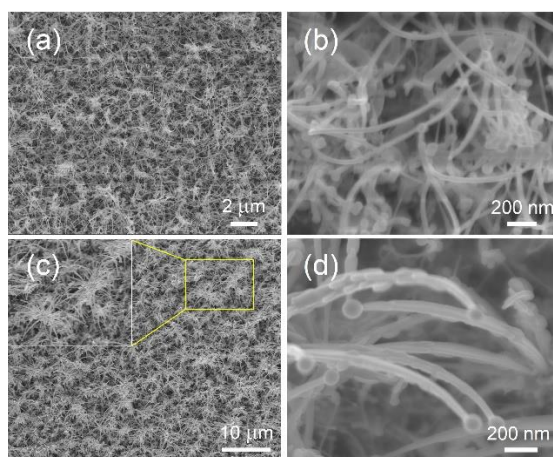


Fig. 2. FE-SEM images of (a, b) pristine ZnO nanowires, (c, d) ZnO-SnO/ZnO Stem/branches nanowires.

The XRD pattern of the as-prepared ZnO product with gold catalyst is shown in Fig. 3a. The pattern with diffraction peaks can be assigned to the hexagonal wurtzite structure of ZnO (JCPDS File No. 01-079-0205). The crystal structure of the synthesized SnO/ZnO branches – ZnO stem was investigated via X-ray diffraction (XRD), and the results are shown in Fig. 3b. The main peaks in the XRD pattern of the as-synthesized biaxial SnO/ZnO NWs can be indexed to a rutile structure of SnO, which is in good agreement with a standard profile of SnO crystals (JCPDS, No. 01-085-0712). In addition to the SnO diffractions, broad diffraction peaks from the (100), (002) and the (101) lattice planes of ZnO were also identified (JCPDS, No. 01-079-0205). Beside the main peaks from SnO and ZnO, four characteristic peaks of metal Sn are identified, and are indexed to be the (200), (101), (220), and (211) reflections from Sn. Fig. 3b shows that the diffraction peaks of SnO phase are stronger and sharper than those of ZnO, which indicate that SnO NWs have a higher crystallinity than ZnO. The morphology of the as-synthesized product after second step is shown in Fig. 2(c, d). Fig. 2c shows a low-magnification image with a uniform feature consisting of branch nanowires grown around of body and top of ZnO stem nanowires. Fig. 2d shows the higher magnification of the sample. It is apparent that the nanowires' diameters gradually decrease from the root (~170 nm) to the tip (70 nm). The nanowires possess

an average length of 5 μm , with spherical balls average diameter of 100 nm on their tips.

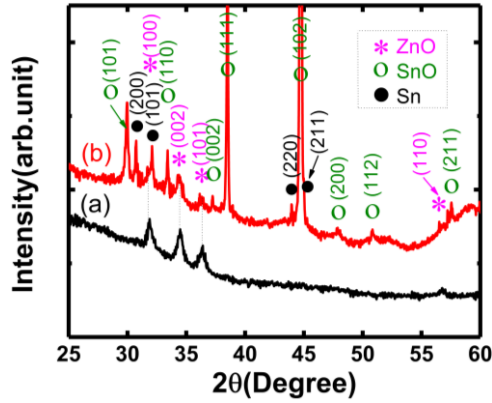


Fig. 3. (a) XRD patterns of ZnO stem nanowires prepared with Au catalyst (after first step). (b) XRD patterns of CVT products obtained at growth temperature of 360°C (after second step).

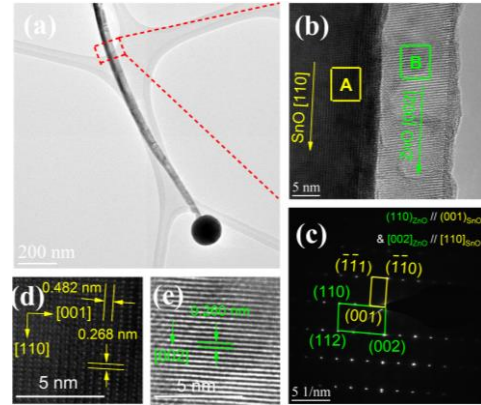


Fig. 4. (a) Low- [(b), (d), (e)] High-resolution TEM images of biaxial nanowire. (c) SAED pattern of region A from the p-SnO part in the Fig. 4(b).

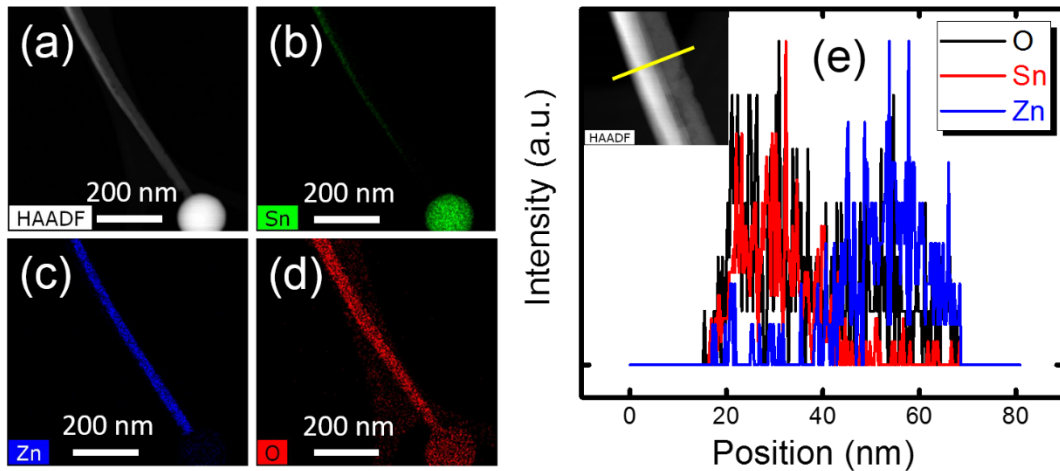


Fig. 5. (a) HAADF-STEM images of the SnO/ZnO biaxial nanowires; (b), (c), (d) The elemental mapping images of Sn, O and Zn for the biaxial nanowire, respectively; (e) The line scan analysis profiles across the entire biaxial nanowire along the yellow line (Insert Fig. 5e).

It is consistent with FE-SEM results (Fig. 2(c, d)), TEM image in Fig. 4a shows the nanowire with conical shapes. The biaxial nanowire can be divided into two regions by the stacking faults, which are clearly distinguished from the contrast difference in the HR-TEM image (Fig. 4b). The HR-TEM image of the area marked by a yellow square (labeled “A”) in Fig. 4b is shown in Fig. 4d confirm lattice spacings of 0.482 nm and 0.268 nm correspond to the (001) and (110) plane of the tetragonal structured of SnO, respectively, and the orientation of SnO nanowires along [110] direction can be

confirmed. The SEAD pattern in Fig. 4c demonstrates the single-crystal nature of SnO nanowire. The HR-TEM image of the area marked by label “B” (green square) in Fig. 4a is shown in Fig. 4e confirm lattice spacings of 0.260 nm which with the (002) planes of the wurtzite structured ZnO. Therefore, the growth direction of ZnO nanowire is possible [002]. The HR-TEM image in Fig. 4b shows the stacking fault of SnO/ZnO interface is parallel to the growth direction of ZnO nanowire of [002] and growth direction of SnO nanowire of [110]. To further disclose the heterostructure characteristic of biaxial structure nanowire, detailed composition analysis in STEM mode is carried out. Fig. 5a display the STEM images of the nanowire, and its corresponding spatially resolved elemental mappings of Sn, Zn, and O elements are presented in Fig. 5(b, c, d), respectively. The spatial distributions of Sn, Zn and O elements of the sample morphologies of SnO/ZnO heterostructure, implying that a SnO/ZnO interface in the biaxial nanowire structure. One can clearly see that the left and right regions are identified as the appearances of SnO and the ZnO phase, respectively. The spherical particle on the tip of the nanowire is composed of Sn and O elements (Fig. 5(b-d)). The line scan analysis profiles across the entire branch nanowire along the yellow line (Fig. 5e) are presented in Fig. 5e, which clearly illustrate the distribution difference of Sn, Zn and O elements inside the biaxial nanowire. This result is also in good agreement with the HR-TEM data (Fig. 4(a, b)).

3.2. Formation mechanism of the biaxial SnO/ZnO nanowires

At present, it seems that the above results mentioned VLS mechanism of growth agrees with the observed presence of alloy Sn-Zn balls at the tips of the biaxial nanowires. We believed that both of SnO nanowire and ZnO nanowire were grown simultaneously on the glass substrate. And this continuous growth will eventually cause SnO vapor sources to become exhausted, lead to a continuous SnO nanowire, cannot be grown while a continuous ZnO vapor can be formed. Although the SnO/ZnO biaxial hetero-nanowires has grown in a cone-like morphology but ZnO wire have a diameter uniform and the neck of biaxial nanowire is ZnO pristine (Fig. 5). It seems that the initial alloy Sn-Zn was formed such as catalyst for growth biaxial SnO/ZnO nanowire. This anticipation can be strengthened by the fact that there were no ball and no nanowires produced if we only use pure SnO powder under otherwise similar conditions (800°C, 3×10^{-5} Torr). It is, therefore, interesting to find out what has happened in the Sn-Zn ball during the heating and how it provides the precursor to produce the Sn, Sn-Zn, SnO and ZnO source at low temperature (360°C). It is known that Sn can be provide from the disproportional reaction of SnO [28] as follows:





Moreno et al. reported that this two-step reaction can take place above 300°C, with the fastest rate achieved in the temperature range of 400-500°C [29]. Previous studies showed that the decomposition of SnO₂ occurred at high temperature and strongly depends on the pressure of oxygen according to reaction (3) below [30-32].



The appearance of SnO(g) may also lead to the formation of SnO₂ and Sn through the following reaction [33].



Our previous study [10] showed that reaction (3) and reaction (4) are thought likely to be responsible for the formation of Sn(l), SnO(g), SnO₂(s), and O₂(g). Based on the above analysis, a self-catalytic VLS growth of the biaxial SnO/ZnO nanowire is suggested, as shown in the schematics of Fig. 6. Fig. 6(a-b) shown the schematic diagram of the growth for ZnO stem nanowire in step 1. In the step 2, the SnO/ZnO branched biaxial nanowires were fabricated through co-evaporation of ZnO with a small amount (from the buffer layer under the ZnO nanowire film which was formed in step 1) of SnO powder source. The growth of the biaxial SnO/ZnO nanowire presented in the present study can be separated into three stages. In the first stage, when the evaporating temperature increases up to 800°C, ZnO (buffer layer - Fig. 6b) evaporate and move in the center region of quartz tube and react with Sn vapor which was formed from reaction 1, reaction 2 and reaction 4, lead to formation Zn metal vapor from reaction 5 [34].

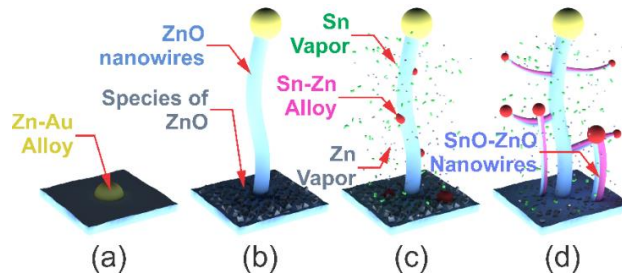


Fig. 6. Schematic diagram of the grown process of the ZnO/SnO biaxial nanowire with Sn-Zn alloy as a catalyst on a ZnO nanowire as a substrate. (a, b) the ZnO nanowire grown on glass substrate with Au catalyst in the first step; (c) Sn species formed from decomposition of SnO₂ and collide with Zn formed Sn-Zn alloy as a catalyst, were adhered on the ZnO nanowire; (d) the growth of ZnO/SnO biaxial nanowire on ZnO nanowire.

Subsequently, Zn combines with Sn to produce Sn-Zn alloy in the second stage. Therefore, the Sn-Zn alloyed can be move and condense again right on the original position at 360°C such catalyst for growth SnO/ZnO biaxial nanowire in a VLS [35].

These Sn-Zn alloyed collided and adhered formed ZnO stem nanowire surface forming Sn-Zn alloyed nanodroplets, as shown in Fig. 6c.

The third stage is the growth process of the SnO/ZnO biaxial nanowires. These Sn-Zn alloyed nanodroplets provide energetically favored sites for absorption of Zn species (Fig. 6c). When the Sn-Zn alloyed droplets are over saturated, the Zn present on the Sn-Zn alloyed droplets may have been oxidized by oxygen decomposed from SnO₂ (reaction 3), and ZnO is formed. Continuous diffusion of Zn atoms to the liquid droplets produces the growth of the ZnO nanowire along the [002] direction, as shown in Fig. 6d. Simultaneously, SnO vapor which were formed from the decomposition of SnO₂ (reaction 3), is transported downstream towards on the ZnO nanowires, thereby constituting a Frank-van der Morwe layer-by-layer growth mode, leading to form biaxial SnO/ZnO nanowire (Fig. 6d). Therefore, only ZnO nanowire was observed at the tip after 60 min processing time (Fig. 4a; Fig. 5(b-c)).

4. Conclusion

In summary, the heterostructure SnO-ZnO biaxial nanowires grown on ZnO nanowire, have been successfully obtained by CVD method at low growth temperature (360°C) through two-step process. According to the HR-TEM and XRD analysis, the biaxial SnO-ZnO nanowire grew along the direction of SnO [110] and ZnO [002]. The growth of the biaxial SnO/ZnO nanowires was believed to follow the VLS process. The Zn combined with Sn vapor forming Sn-Zn eutectic is the catalyst of the growth. In the present work, the biaxial SnO/ZnO nanowires have been reached in a controlled manner for the synthesis, hopefully it can help us to attain potential applications in nanoscale devices in the future.

Acknowledgement

This research was supported by Le Quy Don Technical University Research Fund No. 20.DH.04, 2020.

References

- [1] X. Liu, D. Wang, and Y. Li, "Synthesis and catalytic properties of bimetallic nanomaterials with various architectures," *Nano Today*, 7, 448-466, 2012.
- [2] L. Y. Liang, Z. M. Liu, H. T. Cao, and X. Q. Pan, "Microstructural, Optical, and Electrical Properties of SnO Thin Films Prepared on Quartz via a Two-Step Method," *ACS Appl. Mater. Interfaces*, 2, 1060-1065, 2010.
- [3] H. Giefers, F. Porsch, and G. Wortmann, "Kinetics of the disproportionation of SnO," *Solid State Ionics*, 176, 199-207, 2005.
- [4] L. Qiang, W. Liu, Y. Pei, G. Wang, and R. Yao, "Trap states extraction of p-channel SnO thin-film transistors based on percolation and multiple trapping carrier conduction," *Solid State Electron*, 129, 163-167, 2017.

- [5] M. Z. Iqbal, F. Wang, H. Zhao, M. Y. Rafique, J. Wang, and Q. Li, "Structural and electrochemical properties of SnO nanoflowers as an anode material for lithium ion batteries," *Scr. Mater.*, 67, 665-668, 2012.
- [6] H. Uchiyama, E. Hosono, I. Honma, H. Zhou, and H. Imai, "A nanoscale meshed electrode of single-crystalline SnO for lithium-ion rechargeable batteries," *Electrochem. Commun.*, 10, 52-55, 2008.
- [7] X. Chu, X. Zhu, Y. Dong, W. Zhang, and L. Bai, "Formaldehyde Sensing Properties of SnO-Graphene Composites Prepared via Hydrothermal Method," *J. Mater. Sci. Technol.*, 31, 913-917, 2015.
- [8] V. X. Hien and Y.-W. Heo, "Effects of violet-, green-, and red-laser illumination on gas-sensing properties of SnO thin film," *Sensors Actuators B Chem.*, 228, 185-191, 2016.
- [9] Z. Cai and J. Li, "Facile synthesis of single crystalline SnO₂ nanowires," *Ceram. Int.*, 39, 377-382, 2013.
- [10] P. T. Hung, V. X. Hien, J.-H. Lee, J.-J. Kim, and Y.-W. Heo, "Fabrication of SnO₂ Nanowire Networks on a Spherical Sn Surface by Thermal Oxidation," *J. Electron. Mater.*, 46, 6070-6077, 2017.
- [11] Zu Rong Dai, and Zheng Wei Pan, and Z. L. Wang, "Growth and Structure Evolution of Novel Tin Oxide Diskettes," *J. Am. Chem. Soc.*, 124, 8673-8680, 2002.
- [12] Y. Hu, K. Xu, L. Kong, H. Jiang, L. Zhang, and C. Li, "Flame synthesis of single crystalline SnO nanoplatelets for lithium-ion batteries," *Chem. Eng. J.*, 242, 220-225, 2014.
- [13] J. H. Shin, J. Y. Song, Y. H. Kim, and H. M. Park, "Low temperature and self-catalytic growth of tetragonal SnO nanobranched," *Mater. Lett.*, 64, 1120-1122, 2010.
- [14] Z. Jia, L. Zhu, G. Liao, Y. Yu, and Y. Tang, "Preparation and characterization of SnO nanowhiskers," *Solid State Commun.*, 132, 79-82, 2004.
- [15] H. Zhang, Q. He, F. Wei, Y. Tan, Q. Jiang, G. Zheng, G. Ding, and Z. Jiao, "Ultrathin SnO nanosheets as anode materials for rechargeable lithium-ion batteries," *Mater. Lett.*, 120, 200-203, 2014.
- [16] Y. Liang, H. Zheng, and B. Fang, "Synthesis and characterization of SnO with controlled flowerlike microstructures," *Mater. Lett.*, 108, 235-238, 2013.
- [17] H. Uchiyama, E. Hosono, I. Honma, H. Zhou, and H. Imai, "A nanoscale meshed electrode of single-crystalline SnO for lithium-ion rechargeable batteries," *Electrochem. Commun.*, 1, 52-55, 2008.
- [18] Z. Su, Y. Zhang, B. Han, B. Liu, M. Lu, Z. Peng, G. Li, and T. Jiang, "Synthesis, characterization, and catalytic properties of nano-SnO by chemical vapor transport (CVT) process under CO-CO₂ atmosphere," *Mater. Des.* 121, 280-287, 2017.
- [19] M. Chen, Z. Huang, G. Wu, G. Zhu, J. You, and Z. Lin, "Synthesis and characterization of SnO-carbon nanotube composite as anode material for lithium-ion batteries," *Mater. Res. Bull.*, 38, 831-836, 2003.
- [20] B. Kumar, D.-H. Lee, S.-H. Kim, B. Yang, S. Maeng, and S.-W. Kim, "General Route to Single-Crystalline SnO Nanosheets on Arbitrary Substrates," *J. Phys. Chem. C.*, 114, 11050-11055, 2010.

- [21] A. J. Mieszawska, R. Jalilian, G. U. Sumanasekera, and F. P. Zamborini, "The Synthesis and Fabrication of One-Dimensional Nanoscale Heterojunctions," *Small*, 3, 722-756, 2007.
- [22] A. Katoch, S.-W. Choi, G.-J. Sun, H. W. Kim, and S. S. Kim, "Mechanism and prominent enhancement of sensing ability to reducing gases in p/n core-shell nanofiber," *Nanotechnology*, 25, p. 175501, 2014.
- [23] C. Lan, J. Gong, and Y. Jiang, "Synthesis and photoluminescence properties of string-like ZnO/SnO nanowire/nanosheet nano-heterostructures," *J. Alloys Compd.*, 575, 24-28, 2013.
- [24] S. Park, G.-J. Sun, C. Jin, H. W. Kim, S. Lee, and C. Lee, "Synergistic Effects of a Combination of Cr₂O₃-Functionalization and UV-Irradiation Techniques on the Ethanol Gas Sensing Performance of ZnO Nanorod Gas Sensors," *ACS Appl. Mater. Interfaces*, 8, 2805-2811, 2016.
- [25] Z. Qu, Y. Fu, B. Yu, P. Deng, L. Xing, and X. Xue, "High and fast H₂S response of NiO/ZnO nanowire nanogenerator as a self-powered gas sensor," *Sensors Actuators B Chem.*, 222, 78-86, 2016.
- [26] P. T. Hung, P. D. Hoat, V. X. Hien, H. Y. Lee, S-W. Lee, J. H. Lee, J. J. Kim, and Y. W. Heo, "Growth and NO₂ sensing properties of biaxial p-SnO/n-ZnO heterostructured nanowires," *ACS Appl. Mater. Interfaces*, 30, 34274-34282, 2020.
- [27] F.-H. Chu, C.-W. Huang, C.-L. Hsin, C.-W. Wang, S.-Y. Yu, P.-H. Yeh, and W.-W. Wu, "Well-aligned ZnO nanowires with excellent field emission and photocatalytic properties," *Nanoscale*, 4, 1471-1475, 2012.
- [28] V. X. Hien and Y.-W. Heo, "Sn Spheres Embedded in a SiO₂ Matrix: Synthesis and Potential Application As Self-Destructing Materials," *ACS Appl. Mater. Interfaces*, 8, 21787-21797, 2016.
- [29] M. S. Moreno, R. C. Mercader, and A. G. Bibiloni, "Study of intermediate oxides in SnO thermal decomposition," *J. Phys. Condens. Matter.*, 4, 351-355, 1992.
- [30] E. R. Leite, J. A. Cerri, E. Longo, J. A. Varela, and C. A. Paskocima, "Sintering of ultrafine undoped SnO₂ powder," *J. Eur. Ceram. Soc.*, 21, 669-675, 2001.
- [31] R. Colin, J. Drowart, and G. Verhaegen, "Mass-spectrometric study of the vaporization of tin oxides: Dissociation energy of SnO," *Trans. Faraday Soc.*, 0, 1364-1371, 1965.
- [32] C. L. Hoenig and A. W. Searcy, "Knudsen and Langmuir Evaporation Studies of Stannic Oxide," *J. Am. Ceram. Soc.*, 3, 128-134, 1966.
- [33] M. Nagano, "Growth of SnO₂ whiskers by VLS mechanism," *J. Cryst. Growth*, 66, 377-379, 1984.
- [34] H. Lv, D. D. Sang, H. D. Li, X. B. Du, D. M. Li, and G. T. Zou, "Thermal Evaporation Synthesis and Properties of ZnO Nano/Microstructures Using Carbon Group Elements as the Reducing Agents," *Nanoscale Res. Lett.*, 5, 620-624, 2010.
- [35] M. Hansen and F. A. Shunk, "Constitution of binary alloys; 2nd suppl.," *McGraw-Hill*, 1969.

SỰ HÌNH THÀNH VÀ CẤU TRÚC CỦA DÂY NANO HAI TRỤC SnO/ZnO TRÊN DÂY ZnO DỰA TRÊN CƠ CHẾ HƠI-LÔNG-RẮN

**Phạm Tiến Hưng, Trần Quang Đạt, Nguyễn Xuân Thấu,
Nguyễn Vũ Tùng, Nguyễn Tiến Anh, Phạm Văn Thìn**

Tóm tắt: Trong nghiên cứu này, dây nano hai trục SnO/ZnO chiều dài trung bình 5 micro đã được tổng hợp thành công trên dây ZnO sử dụng hệ lắng đọng pha hơi thông qua một quy trình hai bước. Bước 1, dây ZnO được mọc trực tiếp lên trên đế kính với chất xúc tác vàng. Bước 2, những dây nano này được sử dụng làm khuôn mẫu cho sự phát triển của dây hai trục SnO/ZnO mà không cần bất kỳ chất xúc tác nào. Sản phẩm sau chế tạo được phân tích bằng nhiễu xạ tia X, kính hiển vi điện tử quét (FE-SEM) và kính hiển vi điện tử truyền qua (HR-TEM). Hợp kim Sn-Zn được hình thành trong quá trình bốc bay đóng vai trò chất xúc tác cho quá trình tăng trưởng của dây nano hai trục SnO/ZnO. Cấu trúc hai trục được hình thành do sự phát triển đồng thời của dây nano SnO và ZnO dọc theo hướng của SnO [110] và ZnO [002]. Cơ chế phát triển của dây nano hai trục SnO/ZnO đã được thảo luận. Cấu trúc đã tổng hợp có thể là ứng viên tiềm năng trong ứng dụng cảm biến khí.

Từ khóa: SnO; ZnO; dây hai trục; CVD; VLS.

Received: 09/3/2021; Revised: 27/5/2021; Accepted for publication: 17/9/2021

